Gender-specific impact of trans 10, cis 12-conjugated linoleic acid on pai transgenic female mice

Yu Rao[1,2,#], Luwen Liang[1,#], Meijuan Li[3,#], Yangyang Wang[1], Baozhu Wang[1], Kemian Gou[1,2,*]

[1]*Institute of Comparative Medicine,* [2]*Jiangsu Co-innovation Center for Prevention and Control of Important Animal Infectious Diseases and Zoonoses, College of Veterinary Medicine, Yangzhou University, Yangzhou 225009, China*;

[3]*Institute of Animal Husbandry and Veterinary Science, Guizhou Academy of Agricultural Sciences, Guiyang 550005, China.*

# YR, LL, and ML contributed equally to this work.

*Corresponding author: Kemian Gou, College of Veterinary Medicine, Yangzhou University, Yangzhou 225009, China.

Email: gou@yzu.edu.cn

ABSTRACT

Trans 10, *cis* 12-conjugated linoleic acid (t10c12-CLA) has been shown to induce body fat loss in mammals. In this study, we analysed female pai transgenic mice that produced t10c12-CLA to determine the long-term impact of this substance on the lipid metabolism of lean mammals. Phenotype profiling showed that the effects of t10c12-CLA were genotype-specific in biallelic pai/pai or monoallelic pai/wt mice compared to their wild-type littermates. In both pai genotypes, white fat was not reduced, but heat release was decreased. Specifically, pai/wt mice exhibited increased chronic FGF21 and adrenaline possibly to regulate energy homeostasis and reduce physical activities. Contrarily, pai/pai mice showed hypothermia which may be related to the overproduction of prostaglandins and adrenaline, as well as an inflammatory response. Analysis of brown adipose tissue indicated that hypothermia might conversely promote thermogenesis and lipolysis by up-regulating UCP1/2, pHSL, CPT1B, and AMPK, and down-regulating pAMPK in pai/pai mice. Moreover, pai/pai mice also showed hypertriglyceridemia and fatty liver which is associated with long-term excesses of corticosterone and glucagon. Further analysis of pai/pai livers revealed that hepatic steatosis resulted from attenuated lipid metabolism via down-regulating pAMPK and fatty acid synthase. These results suggest that the systemic impact of chronic t10c12-CLA is dose-dependent in lean female mammals, low doses of t10c12-CLA may play an active role via the FGF21 and/or adrenaline pathways while its high-dose exposure may cause hormones overproduction and pose a safety risk.

Keywords: thermogenesis; FGF21; adrenaline; prostaglandins; corticosterone; glucagon

1. INTRODUCTION

Trans 10, cis 12-conjugated linoleic acid (t10c12-CLA), one of the most studied isomers of linoleic acid, occurs naturally in small amounts in some foods such as beef and dairy products. Its popular health benefit is reducing body fat by increasing energy expenditure and white adipose tissue (WAT) browning [1,2], promoting biosynthesis of N-lactoyl-phenylalanine via the up-regulation of cytosolic nonspecific dipeptidase 2 in WAT [3], or increasing intramuscular fat [4]. In addition, it has other potential health influences, including depressing milk fat production by inhibiting lipogenesis [5-7], reducing the globule size of milk fat droplets [8], protecting against atherosclerosis by modulating the macrophage phenotype [9], promoting beneficial effects on cholesterol efflux [10], reducing oxidative stress [11], changing intestinal microbiota [12] and metabolite profiles [4], down-regulating Alzheimer's hallmarks in an aluminium mouse through an Nrf2-mediated adaptive response and increasing brain glucose transporter levels [13].

Although the potential health benefits, especially the fat loss properties of t10c12-CLA, have been extensively studied, little is known about the mechanism of action of t10c12-CLA and it is also unclear what the optimal dosage for this fatty acid is, particularly under different host obesity or food fat degrees [14,15]. Moreover, some studies have not found its effects on fat reduction, and even a few studies have indicated its side effects result in fatty liver, an inflammatory response, and insulin resistance [11]. As we know, commercial CLA supplements used in most studies contain 10-20% other CLA isomers and the t10c12-CLA-mediated effect might be covered or reversed by other isomers. Additionally, commercial CLA differs significantly in the ratio of cis 9, trans 11-CLA to t10c12-CLA (approximately 1:1) when compared to levels found in food (approximately 8~9:1), therefore, CLA supplement users ingest significantly more t10c12-CLA than would be obtained from the diet [11,16]. This excessive t10c12-CLA dosage or CLA mixture supplements can bring the health impact of t10c12-CLA into conflict.

To identify the individual t10c12-CLA's impacts, we have produced a transgenic mouse that can produce t10c12-CLA by inserting the foreign gene encoding the *Propionibacterium acnes* isomerase (PAI) into the Rosa26 locus (Rao et al, 2023 bioRxiv preprint: https://doi.org/10.1101/2023.01.31.526123). In its lean male offspring, decreased white fat was observed in biallelic pai/pai, not in monoallelic

80 pai/wt genotypes, suggesting t10c12-CLA's impact on fat reduction in a dose-
81 dependent manner. The pai/wt male mice with excess FGF21 in the blood suggests
82 that t10c12-CLA in low doses possibly stimulate the FGF21 secretion and plays an
83 active role via the pathway of FGF21 on health. Whereas the lean pai/pai male mice
84 released more heat by promoting energy expenditure via UCP1/2-mediated
85 thermogenesis and increasing fatty acids oxidation through the CPT1B pathway in
86 brown adipose tissue (BAT) (Rao et al, 2023 bioRxiv preprint:
87 https://doi.org/10.1101/2023.01.31.526123). The study on male mice suggests that fat
88 mass loss is the result of BAT heating, and the pathways of t10c12-CLA action are
89 associated with its dosage.

90 The current study investigated the adiposity characteristics and metabolic
91 profiles of lean pai female mice. In contrast to their male counterparts, the findings of
92 this study demonstrate that pai female mice did not experience changes in body fat,
93 but did experience a decrease in heat release. Moreover, specific metabolic features in
94 female mice indicate that the systemic effects of t10c12-CLA on health are dose-
95 dependent and gender-specific. The results suggest that pai mice may be a useful
96 model to investigate the chronic t10c12-CLA's effects and its mechanisms of action in
97 the body.

2. MATERIALS AND METHODS

2. 1. Chemicals

Unless otherwise stated, all chemicals were purchased from Sigma (USA) or Sinopharm Chemical Reagent Co., Ltd. (Shanghai, China). Restriction endonucleases were purchased from New England Biolabs Inc (USA).

2. 2. Diet

Fresh diets were prepared every month in accordance with formula No. D12450H of OpenSource DIETS™ (10% kcal% fat, Research Diets Inc., NJ, USA) under sterile conditions. The sources of the food-grade ingredients used in the diets are listed in Supplementary Table 1. The fatty acid composition of the diets was spot-checked using gas chromatography to examine the contents of linoleic acid and t10c12-CLA. Each kilogram of the diet contains approximately 20 g of linoleic acid, and no t10c12-CLA was detected in the diet samples.

2. 3. Mice

All animal experiments were conducted in accordance with the guidance provided by the Committee for Experimental Animals of Yangzhou University. The animal study protocol was approved by the Ethics Committee of Yangzhou University (protocol code NSFC2020-SYXY-20 and dated 25 March 2020). The mice were housed in a light-controlled room (12L:12D, lights on at 0700 h) at a temperature of 22-23°C and fed ad libitum with a standard diet containing 10% kcal% fat. For the transgenic founder produced from hybrids embryos of DBA/2 and C57BL/6J, the pai/wt mice were backcrossed to C57BL/6J mice for more than eight generations before the present study. Then the pai/wt matings were used to produce the biallelic pai/pai, monoallelic pai/wt, and wild-type (wt) offspring for this study. Unless otherwise specified, mice of the above three genotypes aged 11-15 weeks were used for analysis in this study.

2. 4. Methods

The methods utilised in this study, including gas chromatography, RNA and proteins analyses, histology, hepatic and blood parameter measurements, intraperitoneal glucose (2g/kg body weight) and insulin (0.5 IU/kg body weight) tolerance tests, and experiments conducted in metabolic cages (Supplementary method), have been previously described in our study of pai male mice (Rao et al, 2023 bioRxiv preprint: https://doi.org/10.1101/2023.01.31.526123). For reviewing convenience, the methods are copied in the Supplementary methods.

2.5. Genotyping

Genotyping was performed using genomic DNA from tail tissues, with the presence of the pai gene being assayed by amplifying the 514-bp pai fragments (forward: 5-taaccatgttcatgccttcttc-3; reverse: 5-caccttgttgtagtgtccgttt-3) and the wt Rosa26 sequence being assayed by amplifying the 605-bp fragments that spanned the insertional site of the Rosa26 locus (forward: 5-ccaaagtcgctctgagttgttatcagt-3; reverse: 5-ggagcgggagaaatggatatgaag-3). PCR amplification was performed for 30 cycles at 94°C for 30 sec, 57°C for 30 sec, and 72°C for 40 sec.

2.6. Measurement of serum estradiol

Three-week-old mice were injected intraperitoneally with 5 IU pregnant mare serum gonadotrophin (Jinmu Biotech Co. Ltd., Wuxi, China), and 48 h later, blood was collected from the orbital vein of anaesthetised mice and used to measure the serum estradiol levels using the E2 ELISA kit (Meimian Industrial Co. Ltd., Jiangsu, China).

2. 5. Statistical analysis.

Statistical analysis was performed with unpaired Student's t-test or one-way ANOVA (Brown-Forsythe and Welch) among wt, pai/wt, and pai/pai mice. All values are presented as mean ± SD. A p-value of < 0.05 was considered statistically significant.

157 **3. RESULTS**

158

159 ***3. 1. Fatty acids analysis***

160 Gas chromatography was used to analyse the compositions of fatty acids
161 (FAs) in the livers, kidneys, hearts, tibialis anterior muscle, and interscapular BAT.
162 The content of t10c12-CLA had increased by 69% in the pai/wt kidneys compared to
163 wt littermates ($p < 0.05$; Table 1). However, the quantities of substrate linoleic acid had
164 decreased in the pai/pai livers by 23% and skeletal muscle by 34%, and had increased
165 by 36% in the pai/wt kidneys ($p < 0.05$; Supplementary Table 2).

166

Table 1. Comparison of t10c12-CLA and circulating factors in wt and pai mice

	wt	pai/wt	pai/pai
t10c12-CLA (µg/g)			
Liver	2.56 ± 3.24 (7)	4.30 ± 4.10 (5)	ND (5)
Kidney	6.50 ± 1.25[a] (5)	11.0 ± 3.65[b] (6)	6.09 ± 0.42[a] (4)
Heart	ND (5)	ND (4)	ND (4)
Skeletal muscle	ND (4)	ND (4)	ND (4)
Brown adipose tissue	22.4 ± 15.9 (4)	29.5 ± 7.5 (4)	29.8 ± 0.5 (4)
Blood/hormonal parameters			
Blood glucose (mM)	7.35 ± 0.70 (12)	7.37 ± 1.18 (15)	7.55 ± 1.35 (13)
Serum insulin (µg/L)	0.21 ± 0.08 (9)	0.27 ± 0.11 (17)	0.32 ± 0.18 (8)
Serum leptin (µg/L)	1.04 ± 0.41 (8)	0.92 ± 0.21 (14)	0.91 ± 0.31 (7)
Serum ghrelin (ng/L)	181 ± 44(7)	225 ± 108 (20)	210 ± 152 (6)
Serum FGF21 (ng/L)	403 ± 29[a] (16)	441 ± 49[b] (10)	421 ± 34[ab] (18)
Serum total cholesterol (µM)	311 ± 40 (17)	324 ± 40 (8)	321 ± 30 (16)
Plasma triglycerides (mg/dL)	107 ± 35[a] (34)	105 ± 27[a] (29)	129 ± 42[b] (29)
Plasma HDL (mg/dL)	48.6 ± 13.9 (34)	47.7 ± 16.2 (29)	52.5 ± 19.6 (29)
Serum free fatty acids (µM)	471 ± 95 (8)	527 ± 79 (16)	517 ± 136 (8)
Serum Estradiol (pM)	71.0 ± 8.8 (15)	64.9 ± 6.8 (7)	68.4 ± 8.1 (15)
Serum prostaglandin E2 (ng/L)	349 ± 33[a] (16)	356 ± 38[ab] (8)	380 ± 38[b] (16)
Serum glucagon (mU/L)	54.3 ± 62.3[a] (20)	55.0 ± 38.4[a] (17)	104 ± 67[b] (16)
Serum cortosterone (µg/L)	7.51 ± 1.27[a] (16)	7.88 ± 1.64[ab] (8)	8.68 ± 1.61[b] (16)
Serum adrenaline (µg/L)	3.01 ± 1.64[a] (7)	10.5 ± 9.4[b] (14)	13.7 ± 7.5[b] (7)
Serum interleukin-6 (ng/L)	24.7 ± 17.7[a] (9)	47.8 ± 27.8[b] (14)	60.6 ± 32.8[b] (6)
Serum TNFα (ng/L)	69.1 ± 54.9[a] (12)	174 ± 161[b] (16)	205 ± 175[b] (13)
Serum C reactive protein (µg/L)	34.3 ± 19.2[a] (16)	49.1 ± 31.4[a] (17)	107 ± 72[b] (10)
Serum LDH (U/L)	2592 ± 646 (7)	2234 ± 627 (7)	2518 ± 454 (6)

Table 1. Comparison of t10c12-CLA and circulating factors in wt and pai mice

	wt	pai/wt	pai/pai

Note: Tissues from 11-week-old mice was analysed by gas chromatography. Blood samples were collected from non-fasted mice at the ages of 3 (only estradiol analysis) or 11~15 weeks. FGF21, fibroblast growth factor 21; HDL, high-density lipoprotein; LDH, Lactate dehydrogenase; ND, not detected; TNFα, tumour necrosis factor alpha. Each value represents the mean ± SD, and the numbers in brackets indicate the size of the tested samples. Different letters in superscript indicate a level of statistical significance of $p < 0.05$.

The contents of other FAs such as myristic (14:0), palmitic (16:0), stearic (18:0), palmitoleic (16:1n-7), cis-vaccenic (18:1n-7), oleic (18:1n-9), arachidonic (20:4n-6), and docosahexaenoic (22:6n-3) acids were changed to varying degrees in one or more tissues (Supplementary Table 2), This suggests that the changes in the content of each FA were genotype- or tissue-specific. Additionally, the amounts of total FAs (mg/g) increased in the pai/wt kidneys (10.2 ± 1.39 versus 13.3 ± 1.69; $p < 0.05$), similar to our previous study in pai/wt male mice (https://doi.org/10.1101/2023.01.31.526123). These results suggest lipopathy in the pai/wt kidney.

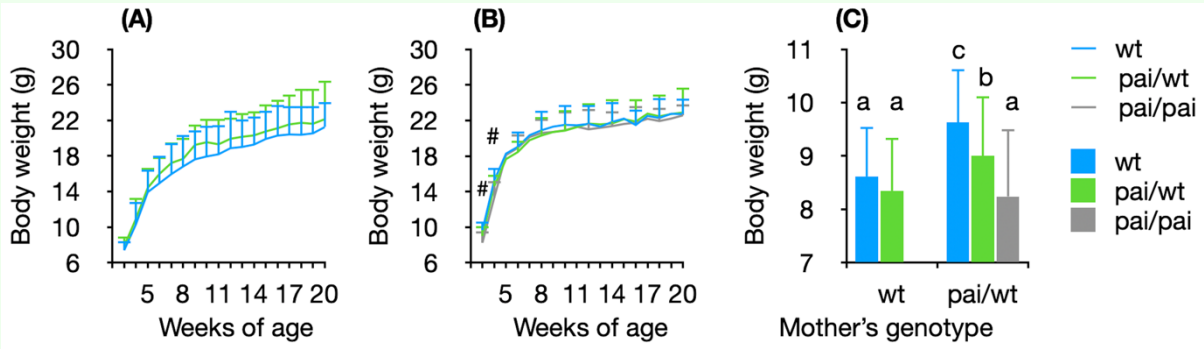

Figure 1. Comparison of growth of pups from wt (A) and pai/wt (B) mothers, as well as their weaning (3-week-old) weight (C). Each group contains 11-29 (A, B) or 24-81 (C) pups. The bars represent the mean ± SD. # or different letters indicate $p < 0.05$ among three genotypes.

3. 2. Body weight analysis

There were no differences in body weight between pai/wt and wt littermates from 3 weeks onwards in the group of wt mothers (Fig. 1A). However, in the group of pai/wt mothers, there was a significant difference in weaning weight among the

185 three genotypes (wt > pai/wt > pai/pai, respectively; $p < 0.05$), and this difference
186 disappeared from five weeks of age onwards (Fig. 1 B-C).

187 Additionally, the weaning weight of wt and pai/wt offspring from pai/wt
188 mothers was higher than that of genotype-matched pups from wt mothers ($p < 0.05$;
189 Fig. 1C), similar to our previous study in male mice (Rao et al, 2023 bioRxiv preprint:
190 https://doi.org/10.1101/2023.01.31.526123). This further confirms that maternal
191 t10c12-CLA may play an active role in developing embryos and/or weaning pups.

192

193 ***3. 3. Energy metabolism and activity studies***

194 Energy metabolism and activity parameters were assessed in consideration of
195 body weight. Compared to their wt littermates, both pai/wt and pai/pai mice
196 exhibited no significant differences in body weight gain, food and water intake (Fig. 2
197 A-C), respiratory exchange ratio (Fig. 2 F-G), and total distance travelled during the
198 whole 72-h observation (Fig. 2 R). However, the other parameters showed varying
199 differences.

200 The pai/pai mice did not decrease their total locomotor activities in either the
201 centre (Fig. 2 J-K, N-O) or margin/corners (Fig. 2 L-M, P-Q). Nevertheless, during both
202 the light ($p < 0.05$) and dark ($p > 0.05$) periods, they consumed 8.9% and 9.2% less O_2
203 (Fig. 2 D) and produced 10.8% and 10.1% less CO_2 (Fig. 2 E) as well as 9.3% and 9.4%
204 less heat (Fig. 2 H-I), respectively. Additionally, pai/pai mice covered a longer
205 distance per sampling duration (~50% longer) and exhibited 52.5% higher speed
206 during the light phase ($p < 0.05$; Fig. 2 S-T). The results suggest that pai/pai mice
207 simultaneously reduce oxygen consumption and heat release while maintaining
208 normal locomotor activities.

209 On the other hand, pai/wt females did not reduce their central activities ($p >$
210 0.05; Fig. 2 J-K) but displayed 30.1% fewer marginal activities, such as marginal
211 ambulating and stereotypic activities during the dark period ($p < 0.05$; Fig. 2 L-M, P-
212 Q). Moreover, during both the light and dark periods, they consumed 10.7% and
213 14.6% less O_2, produced 9.7% and 15.2% less CO_2, as well as 10.5% and 14.7% less heat,
214 respectively ($p < 0.05$, Fig. 2 D-E, H-I), suggesting that pai/wt mice simultaneously
215 reduce oxygen consumption and heat release while exhibiting fewer marginal
216 activities.

217

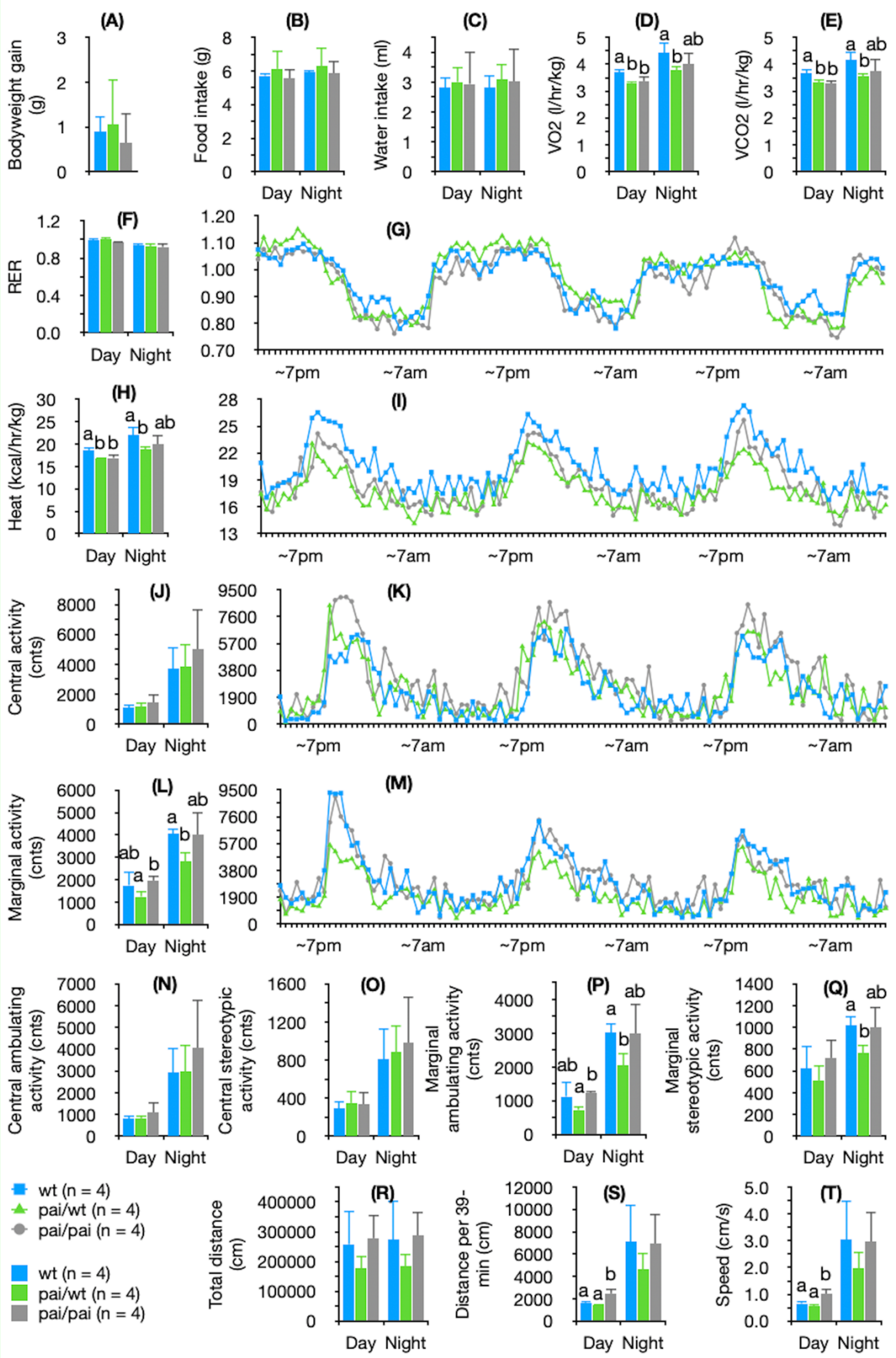

218 **Figure 2. Abnormal energy metabolism and activities in pai mice.** Comparison of body

219 weight gain during a 72-h period (A), food intake (B), water intake (C), O_2 consumption (D),
220 CO_2 production (E), respiratory exchange ratio (RER) and RER time course (F-G), heat release
221 and its time course (H-I), locomotor activities in the centre of the cage and its time course (J-
222 K), locomotor activities in the margin or corners of the cage and its time course (L-M), central
223 ambulating and stereotypic activities (N-O), marginal ambulating and stereotypic activities (P-
224 Q), total distance travelled during a 72-h period (R), distance travelled during a 39-min
225 sampling duration (S), and speed (T) among wt (n = 4), pai/wt (n = 4) and pai/pai (n = 4) mice
226 at 11 weeks. The lights turned on and off at 7:00 am and 7:00 pm, respectively. The data are
227 normalised to lean body weight. The bars represent the mean ± SD. Different letters indicate p
228 < 0.05 within the same phase.

229

230 ***3. 4. Metabolic complications***

231 Concentrations of circulating glucose, insulin, leptin, and ghrelin (Table 1), as
232 well as small intestine length (Supplementary Table 3), showed no significant
233 differences ($p > 0.05$) between pai mice and their wt littermates. This suggests that
234 t10c12-CLA did not have any significant impact on energy intake, which is consistent
235 with the observation in the metabolic cage.

236 Both glucose and insulin tolerance tests showed no difference in the
237 circulating glucose concentrations or the area under the curve between wt and two
238 pai genotypes, however, the glucose levels before glucose injection were significantly
239 ($p < 0.05$) higher in pai/wt mice compared to wt or pai/pai littermates (Fig. 3 A-B).
240 To investigate further, we measured blood glucose levels during a 24-h fasting
241 duration and found that pai/wt mice maintained higher glucose levels continuously
242 compared to their wt littermates ($p < 0.05$; Fig. 3 C). This suggests that t10c12-CLA can
243 ameliorate the circulating glucose level in pai/wt mice during starvation, which may
244 be associated with the elevated FGF21 exclusively in pai/wt mice (Table 1), for its
245 beneficial insulin-sensitising and glucose-lowering effects [17].

246 Although the circulating levels of total cholesterol, free FAs, high-density
247 lipoprotein (HDL), and estradiol showed no significant differences among the three
248 genotypes, the levels of plasma triglycerides (TGs) were significantly elevated in
249 pai/pai mice when compared to wt or pai/wt genotypes ($p < 0.05$, Table 1), indicating
250 hypertriglyceridemia in pai/pai mice.

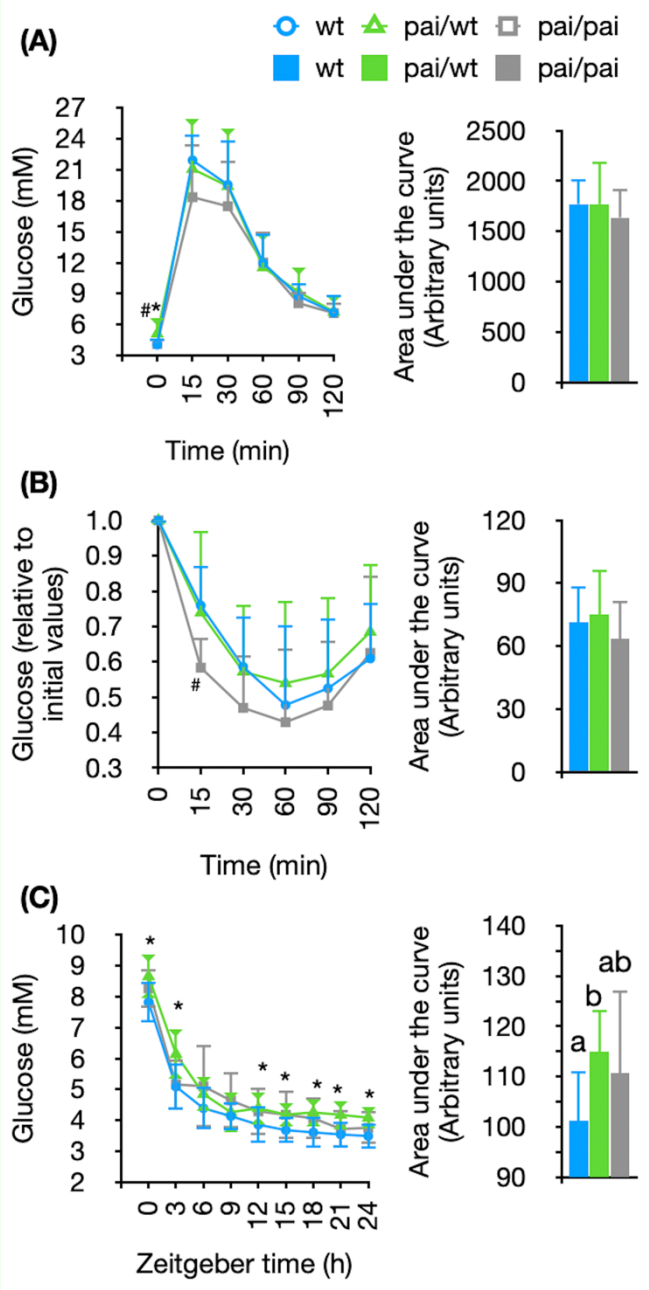

Figure 3. Comparisons of glucose (A) and insulin (B) tolerance tests, and dynamic glucose levels (C) in wt and pai mice. (A) Absolute blood glucose levels and the area under the curve are compared among wt (n = 5), pai/wt (n = 10), and pai/pai (n = 5) mice. (B) Blood glucose levels relative to initial values and the area under the curve are compared among wt (n = 10), pai/wt (n = 12), and pai/pai (n = 7) mice. (C) Dynamic blood glucose levels and the area under the curve are measured in wt (n = 12), pai/wt (n = 13), and pai/pai (n = 10) fasting mice starved from Zeitgeber time 0 to 24. Zeitgeber times 0 and 12 are lights-on and -off times, respectively. The bars represent the mean ± SD. # indicates $p < 0.05$

between wt and pai/pai mice; * indicates $p < 0.05$ between wt and pai/wt mice; #* indicates $p < 0.05$ between pai/wt and wt or pai/pai mice.

In pai/pai mice, serum concentrations of prostaglandin E2 (PGE2, 109%), glucagon (2-fold), corticosterone (116%), adrenaline (4.5-fold), tumour necrosis factor-alpha (TNFα, 3-fold), interleukin-6 (IL-6, 2.5-fold), and C-reactive protein (CRP, 3-fold) were significantly increased ($p < 0.05$; Table 1) when compared to their wt littermates. However, only FGF21 (109%), adrenaline (3.5-fold), TNFα (2.5-fold), and IL-6 (2-fold) were significantly ($p < 0.05$) elevated in pai/wt mice. Additionally, there was no increase in blood levels of lactic acid dehydrogenase in either pai mice, indicating no cellular injury caused by the PAI protein. These results suggest that the t10c12-CLA can lead to an inflammation reaction and response to illness-related stimuli in female mammals.

3. 5. WAT characteristics

WAT features were determined in the mice at 11 weeks of age. Compared to their wt littermates, pai/pai mice showed generalised organomegaly, including significantly enlarged livers, spleens, hearts, and ovaries, when body weight was considered ($p < 0.05$; Supplementary Table 3). However, no fat mass loss was observed (Fig. 4 A-B). The histological analysis did not reveal any changes in the cross-sectional area of white adipocytes (Fig. 4 C-D). Pai/wt mice showed enlarged ovaries only and no fat loss whereas its cross-sectional area per adipocyte was increased ($p < 0.05$), which was also confirmed by the increased mRNA level of leptin (Fig. 4 E).

As shown in Table 2, among 33 examined genes, RNA levels of 14 (42%) genes, including seven up-regulated and seven down-regulated, were changed in pai/pai adipocytes. The names of these genes are listed in Table 2. The seven up-regulated genes were corticosterone receptor Nr3c1, F4/80, Adiponectin, G6p, Fasn, Ppar-γ, and Hsl. The seven down-regulated genes were Lpl, Cpt1a, Plin1, Prdm16, Insr, Glut4, and Chrebp. These aberrant gene expressions in white adipocytes suggest that t10c12-CLA can affect a series of metabolic processes, such as lipid metabolism, lipid and glucose uptake, energy expenditure, stimuli response and glucose homeostasis.

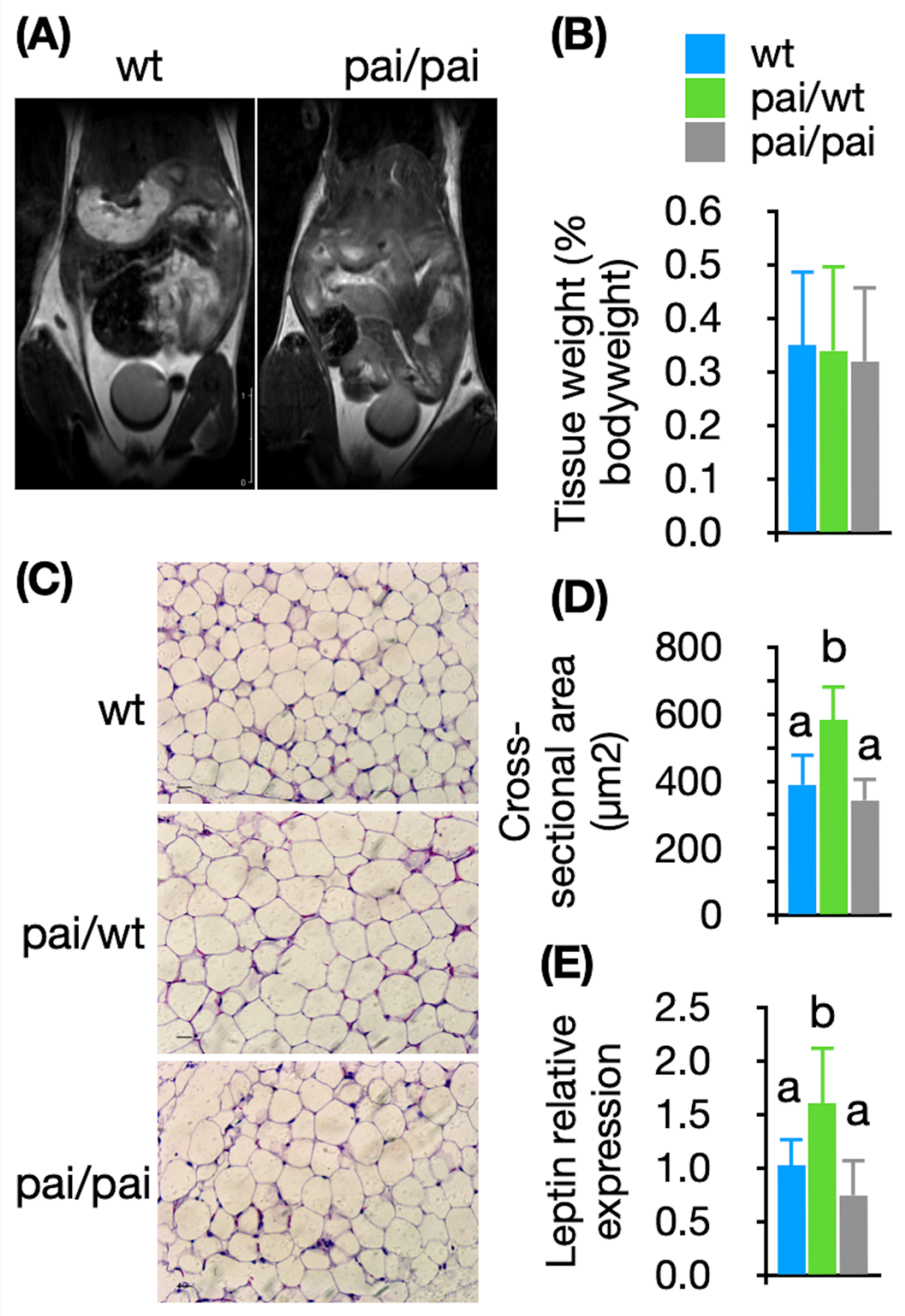

Figure 4. Magnetic resonance imaging and histological analysis of white adipose tissues. (A) Coronal sections were obtained on the whole-body midsection for four wt or pai/pai mice at 11 weeks in each group during magnetic resonance imaging (bar = 1 cm). The wt mice show adipose tissue in the subcutaneous and intra-abdominal regions as areas of increased signal intensity on images. The pai/pai mice show normal body fat. (B) There is no difference in WAT mass among wt (n = 21), pai/wt (n = 17), and pai/pai (n = 13) mice. (C) Imaging of

299 hematoxylin-eosin staining (bar = 10 μm), (D) analysis of cross-sectional area per cell, and
300 (E) RNA level of leptin gene show that the volume of white adipocytes is increased in pai/wt
301 mice (n = 5). The bars represent the mean ± SD. Different letters indicate $p < 0.05$.

302

Table 2. Relative Expression of mRNAs in the white adipose tissue

Genes	wt	pai/pai
Fatty acid synthase (*Fasn*)	1.04 ± 0.30 (6)	1.80 ± 0.47*** (8)
Peroxisome proliferator-activated receptor-γ (*Ppar-γ*)	1.03 ± 0.24 (12)	1.54 ± 0.61* (10)
Adipose triglyceride lipase (*Atgl*)	1.01 ± 0.16 (7)	1.06 ± 0.19 (7)
Hormone-sensitive lipase (*Hsl*)	1.02 ± 0.23 (9)	1.44 ± 0.29* (8)
Monoacylglycerol lipase (*Mgl*)	0.93 ± 0.25 (9)	0.99 ± 0.32 (8)
Perilipin 1a (*Plin1*)	1.07 ± 0.44 (8)	0.43 ± 0.16** (8)
Comparative gene identification 58 (*Cgi58*)	1.04 ± 0.30 (8)	0.81 ± 0.35 (8)
Lipoprotein lipase (*Lpl*)	1.03 ± 0.27 (14)	0.69 ± 0.24** (15)
Carnitine palmitoyltransferase Ia (*Cpt1a*)	1.06 ± 0.36 (8)	0.56 ± 0.15** (8)
Long-chain acyl-CoA dehydrogenase (*Lcad*)	1.12 ± 0.58 (7)	0.95 ± 0.44 (8)
Medium-chain acyl-CoA dehydrogenase (*Mcad*)	1.01 ± 0.17 (6)	1.07 ± 0.18 (9)
Uncoupling protein 1 (*Ucp1*)	1.09 ± 0.50 (6)	5.39 ± 5.88 (7)
Ppar-gamma coactivator 1 alpha (Pgc1α)	1.05 ± 0.39 (8)	1.18 ± 0.37 (8)
PR domain containing 16 (*Prdm16*)	1.01 ± 0.17 (7)	0.70 ± 0.20** (7)
Insulin receptor (*Insr*)	1.03 ± 0.25 (11)	0.75 ± 0.22** (13)
Insulin receptor substrate-1 (*Irs1*)	0.98 ± 0.32 (15)	1.03 ± 0.34 (20)
Insulin receptor substrate-2 (*Irs2*)	1.17 ± 0.69 (5)	2.28 ± 1.29 (6)
Phosphoinositide 3-kinase (*Pi3k*)	1.05 ± 0.39 (5)	0.78 ± 0.37 (8)
IGF binding protein 1 (*Igfbp1*)	1.80 ± 2.00 (6)	0.55 ± 0.14 (5)
Glucose transporter type 4 (*Glut4*)	1.02 ± 0.24 (6)	0.72 ± 0.17* (6)
Carbohydrate response element binding protein (Chrebp)	1.11 ± 0.51 (8)	0.35 ± 0.17** (8)
Fibroblast growth factor 21 (*Fgf21*)	1.08 ± 0.46 (6)	0.71 ± 0.39 (7)
Glucose-6-phosphatase (*G6p*)	1.24 ± 0.87 (6)	2.68 ± 0.83* (6)
Phosphoenolpyruvate carboxykinase (*Pepck*)	1.07 ± 0.42 (8)	1.11 ± 0.42 (8)
AMP-activated protein kinase (*Ampk*)	1.10 ± 0.49 (5)	1.45 ± 0.58 (8)
Leptin	1.03 ± 0.26 (5)	0.75 ± 0.34 (6)
Adiponecin	0.99 ± 0.24 (9)	1.42 ± 0.38** (10)
Nuclear receptor subfamily 3 group C member 1 (*Nr3c1*)	1.04 ± 0.29 (22)	1.64 ± 0.81** (22)
F4/80	1.03 ± 0.29 (12)	1.54 ± 0.58* (11)
CD68	1.06 ± 0.38 (14)	1.03 ± 0.61 (13)
CD11c	1.05 ± 0.29 (14)	0.95 ± 0.44 (16)
CCAAT/enhancer-binding-protein beta (*Cebp*)	1.04 ± 0.31 (6)	1.13 ± 0.60 (8)
Forkhead box protein c2 (*Foxc2*)	1.02 ± 0.21 (5)	1.15 ± 0.45 (7)
Pai	1.24 ± 1.23 (23)	393 ± 270*** (25)

Numbers in brackets indicate the size of tested samples. Each value represents the mean ± SD. * indicates $p < 0.05$; ** indicates $p < 0.01$; *** indicates $p < 0.001$, respectively.

303

304 Similar to pai/pai cells, Ppar-γ (1.52 ± 0.34, n = 10), Nr3c1 (1.53 ± 0.21, n = 12),
305 and F4/80 (1.98 ± 0.64, n = 10) were also up-regulated ($p < 0.05$), and Cpt1a (0.58 ±
306 0.27, n = 5) and Chrebp (0.43 ± 0.45, n = 5) were down-regulated in pai/wt adipocytes
307 compared to wt samples ($p < 0.05$), respectively. The RNA levels of Fasn and
308 Adiponectin were not different from those of wt samples ($p > 0.05$).

309

310 ***3. 6. BAT thermoregulation***

311 To investigate the possible reason for hypothermia in pai/pai mice, BAT
312 features were measured. Magnetic resonance imaging and dissection analysis did not
313 reveal any mass changes of BAT in pai mice (Fig. 5 A-B). HE staining showed pai/pai
314 adipocytes with uniform and small-sized lipid drops, while pai/wt adipocytes had
315 size-irregularly lipid drops compared to wt adipocytes containing uniform and large-
316 sized lipid drops (Fig. 5 C). The reduced cross-sectional areas per adipocyte indicated
317 that the volumes of brown adipocytes decreased significantly in both pai genotypes
318 ($p < 0.05$; Fig. 5 D).

319 In pai/pai brown adipocytes, among the 18 tested genes, the transcriptional
320 levels were changed in eight genes, which were up-regulated Fasn, Atgl, Plin1, Fgf21,
321 and Ampk; as well as down-regulated Hsl, Mgl, and Pgc1α ($p < 0.05$; Fig. 5 E). In
322 contrast, the other critical genes involved in lipolysis and thermogenesis, such as Ppar-
323 γ, Ucp1, Ucp2, Prdm16, and Ppar-δ, showed no changes in RNA levels. Western blot
324 analysis revealed that UCP1 and UCP2, phosphorylated HSL and CPT1B were over-
325 expressed ($p < 0.05$; Fig. 5 F-G). Simultaneously, an increase in total AMPK and a
326 decrease in phosphorylated AMPK were observed in pai/pai BAT. These results
327 indicate that the t10c12-CLA effect is associated with BAT's thermogenesis, lipolysis,
328 and beta-oxidation processes. The discrepancy of levels of some mRNA and their
329 encoded proteins also suggests the complex regulation by feedback or adaptive
330 response.

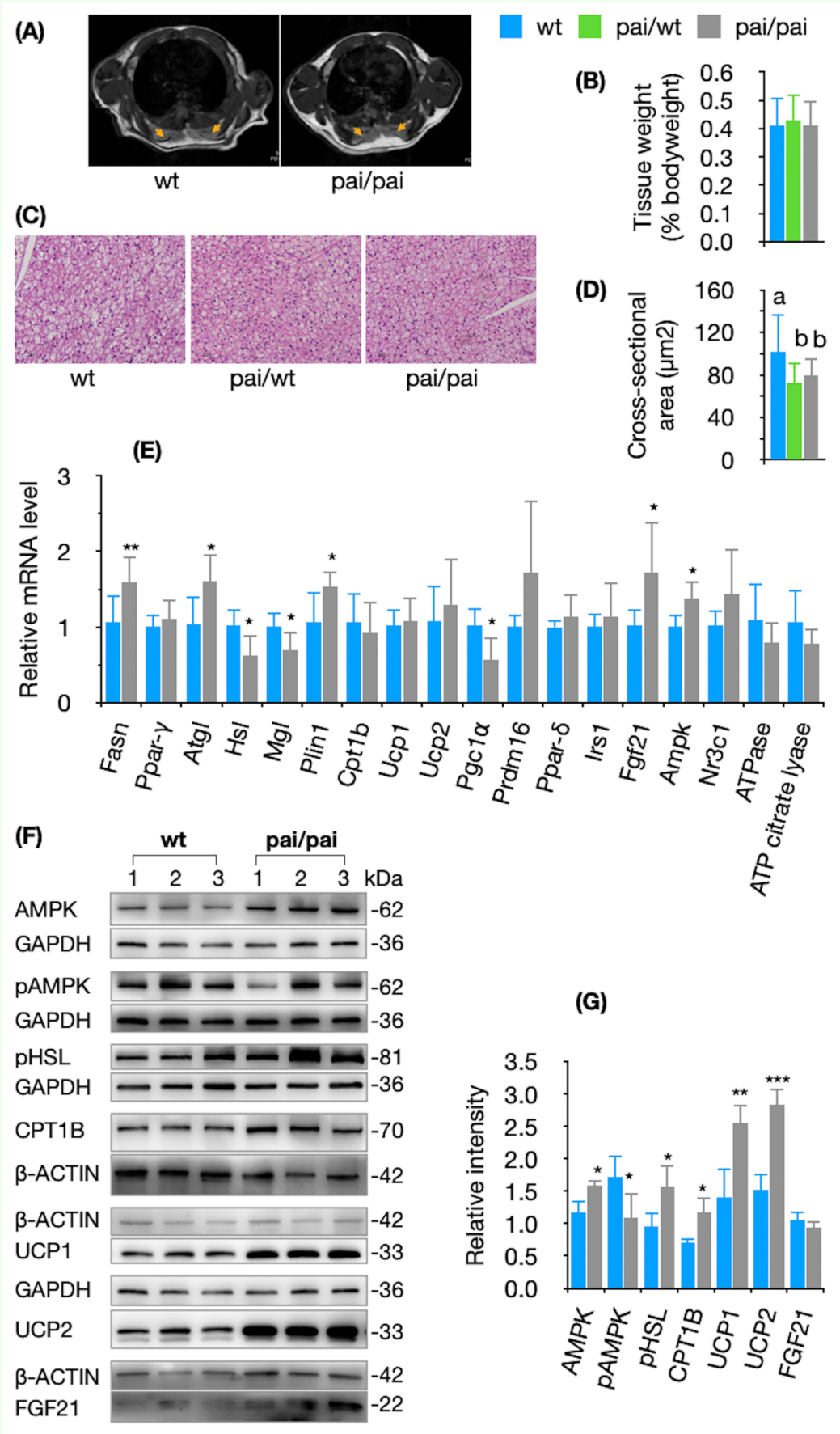

331 **Figure 5. Aspects of brown adipose tissues.** (A) Axial sections of the interscapular BAT

332 show similar areas of grey signal intensity on magnetic resonance images (brown arrows)
333 between four pai/pai and four wt mice at 11 weeks. (B) There is no BAT mass difference among
334 wt (n = 21), pai/wt (n = 17), and pai/pai (n = 13) mice. (C-D) Analysis of hematoxylin-eosin
335 staining shows that the sizes of lipid drop become small in the pai/wt or pai/pai adipocytes (bar
336 = 10 μm) and the cross-sectional area per cell is decreased in pai/wt and pai/pai mice (n = 5).
337 (E) Analyses of the relative expression of mRNAs of critical genes in wt (n = 5~6) and in
338 pai/pai (n = 6~8) mice. (F-G) Western blot analysis of proteins and their relative intensities in
339 wt and pai/pai mice (n = 3). The full name of the gene/proteins is listed in Table 2. pAMPK,
340 phosphorylated AMPK; pHSL, phosphorylated hormone-sensitive lipase. The bars represent
341 the mean ± SD. Different letters or * indicate $p < 0.05$; ** indicates $p < 0.01$; *** indicates $p <$
342 0.001, respectively.

343

344 ***3. 7. Hepatic features***

345 To investigate if t10c12-CLA affects hepatic function, we compared the pai
346 liver features and the molecular basis of lipid and glucose metabolism with wt
347 samples.

348 In pai/pai mice, hepatic hypertrophy was observed (Fig. 6 A). The levels of
349 hepatic TC remained unchanged (Fig. 6 B), but the transcriptional levels of critical
350 genes involved in the sterol pathway were changed, which were down-regulated
351 Srebp1a, Insig2, Hmgcr, and Ldlr; as well as up-regulated Srebp1c and Insig1 ($p <$
352 0.05; Table 3). On the other hand, the levels of hepatic TGs increased by 15.4%, and
353 histological staining showed profound fat accumulation (~2.3 fold) in swollen
354 hepatocytes ($p < 0.05$; Fig. 6 C-F), indicating hepatic steatosis in pai/pai mice. RNA
355 levels of 40% (10/22) genes involved in lipid metabolism were significantly ($p < 0.05$)
356 altered in pai/pai livers, including two up-regulated (Mgl and Cgi58) and eight down-
357 regulated genes, which were down-regulate Ppar-γ, Dgat1, Dgat2, Atgl, Lpl, Cpt1a,
358 Mcad, and Acox1; as well as up-regulated Mgl and Cgi58 (Table 3). Western blot
359 analysis revealed that the protein levels of pAMPK and FASN were reduced and
360 CPT1A was increased while the levels of AMPK, ATGL, and CPA1B did not change
361 (Fig. 6 H-I). The result indicates that the chronic effect of t10c12-CLA attenuates the
362 pathway modified by pAMPK. It also suggests that hepatic steatosis causes the down-
363 regulation of fatty acid synthesis and up-regulation of beta-oxidation through
364 negative feedback in the liver.

365 Moreover, this study analysed a range of crucial enzymes related to
366 insulin/IGF signalling and glucose metabolism. The mRNA levels of Igfbp1, Glut4,
367 Fgf21, G6p, and Pepck were decreased, but western blot analysis showed that the
368 FGF21 level did not alter. These findings suggest that t10c12-CLA may have a
369 significant impact on glucose metabolism and insulin sensitivity at least on
370 transcriptional levels in female livers. Additionally, two NADPH-producing
371 enzymes, Malic and Pgd, were significantly up-regulated, and the inflammatory
372 factor CD11c was down-regulated in the pai/pai livers ($p < 0.05$; Table 3).

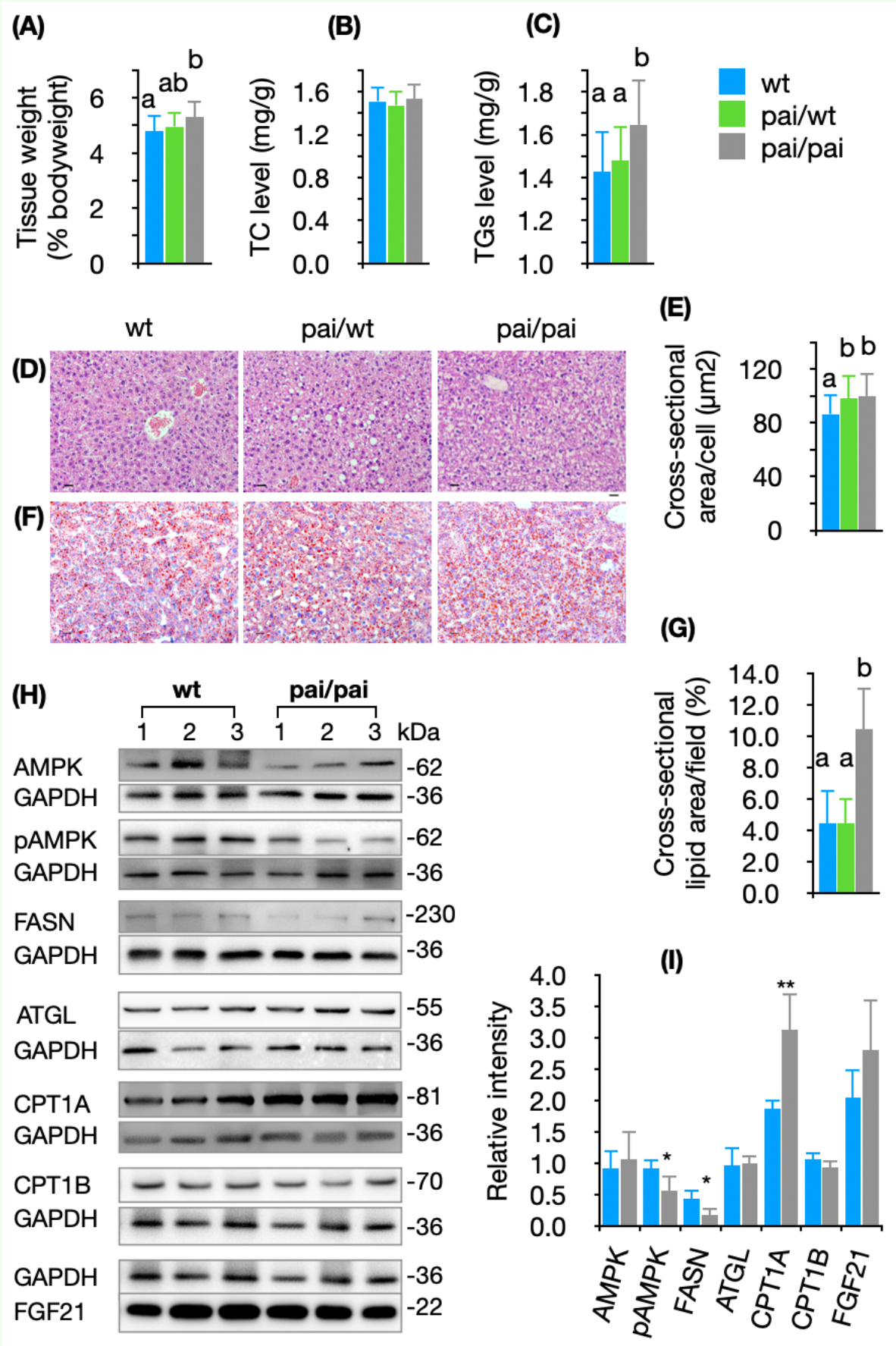
(A)
Tissue weight (% bodyweight)
6
4
2
0
a
ab
b
(B)
TC level (mg/g)
1.6
1.2
0.8
0.4
0.0
(C)
TGs level (mg/g)
1.8
1.6
1.4
1.2
1.0
a a
b
wt
pai/wt
pai/pai
wt
pai/wt
pai/pai
(D)
(F)
(E)
Cross-sectional area/cell (μm2)
120
80
40
0
a
b b
(G)
Cross-sectional lipid area/field (%)
14.0
12.0
10.0
8.0
6.0
4.0
2.0
0.0
a a
b
(H)
wt
pai/pai
1 2 3 1 2 3 kDa
AMPK -62
GAPDH -36
pAMPK -62
GAPDH -36
FASN -230
GAPDH -36
ATGL -55
GAPDH -36
CPT1A -81
GAPDH -36
CPT1B -70
GAPDH -36
GAPDH -36
FGF21 -22
(I)
Relative intensity
4.0
3.5
3.0
2.5
2.0
1.5
1.0
0.5
0.0
*
*
**
AMPK
pAMPK
FASN
ATGL
CPT1A
CPT1B
FGF21

373

374 **Figure 6. Lipid and histological analysis of livers.** (A) Dissection analysis shows increased
375 liver mass in pai/pai (n = 13) but not in pai/wt (n = 17) mice compared to wt mice (n = 21). (B-
376 C) ELISA analyses indicate similar levels of hepatic total cholesterol (TC) and the increased
377 levels of triglycerides (TGs) in pai/pai livers (n = 12) compared to wt (n = 14) and pai/wt (n =
378 14). (D-E) Analyses of hematoxylin-eosin staining show the abnormal morphology and
379 hepatocyte oedema in pai/pai livers, and the enlarged cross-sectional area per cell in pai/pai
380 and pai/wt hepatocytes compared to wt samples (n = 5). (F-G) Analyses of Oil red staining
381 show hepatic lipid accumulation in pai/pai but not in pai/wt mice compared to wt mice (n = 5),
382 Bar = 10 μm. (H-I) Western blot analysis of proteins and their relative intensities in wt and
383 pai/pai mice (n = 3). The bars represent the mean ± SD. Different letters or * indicate $p < 0.05$,
384 ** indicates $p < 0.01$, respectively.

385

Table 3. Relative Expression of mRNAs in the liver

Genes	wt	pai/wt	pai/pai
Sterol pathway			
Liver X receptor α (*Lxrα*)	1.00 ± 0.09 (6)	0.91 ± 0.26 (6)	1.08 ± 0.45 (8)
Liver X receptor β (*Lxrβ*)	1.04 ± 0.31 (9)	0.91 ± 0.42 (6)	1.11 ± 0.26 (7)
SREBP cleavage-activating protein (*Scap*)	1.01 ± 0.15 (8)	0.92 ± 0.15 (6)	0.90 ± 0.25 (6)
Sterol Regulatory Element Binding Protein-1a (*Srebp1a*)	1.02 ± 0.22[a] (7)	0.46 ± 0.25[b] (6)	0.61 ± 0.20[b] (7)
Srebp1c	0.96 ± 0.33[a] (6)	1.61 ± 0.55[b] (7)	1.60 ± 0.42[b] (5)
Srebp2	1.07 ± 0.39 (8)	1.06 ± 0.22 (7)	1.25 ± 0.52 (8)
Insulin induced gene 1 (*Insig1*)	1.03 ± 0.25[a] (7)	1.97 ± 0.52[b] (7)	1.47 ± 0.26[b] (5)
Insulin induced gene 2a (*Insig2*)	1.07 ± 0.38[a] (6)	0.20 ± 0.34[b] (6)	0.59 ± 0.31[b] (5)
HMG-CoA reductase (*Hmgcr*)	1.01 ± 0.16[a] (6)	1.23 ± 0.32[a] (5)	0.62 ± 0.34[b] (6)
LDL receptor (*Ldlr*)	1.04 ± 0.33[a] (8)	1.23 ± 0.36[a] (6)	0.71 ± 0.10[b] (5)
Fatty acid and TGs synthesis			
Stearoyl-CoA desaturase 1 (*Scd1*)	1.07 ± 0.43 (7)	0.97 ± 0.49 (6)	1.11 ± 0.57 (6)
Peroxisome proliferator-activated receptor-γ (*Ppar-γ*)	1.01 ± 0.46[a] (14)	1.06 ± 0.27[a] (7)	0.66 ± 0.44[b] (12)
Glycerol-3-phosphate acyltransferase 1 (*Gpat1*)	1.04 ± 0.33 (7)	1.44 ± 0.46 (6)	1.22 ± 0.31 (6)
1-acylglycerol-3-phosphate O-acyltransferase 2 (*Agpat2*)	0.97 ± 0.25 (8)	0.80 ± 0.22 (6)	1.11 ± 0.31 (7)
Diacylglycerol acyltransferase-1 (*Dgat1*)	1.00 ± 0.16[a] (7)	0.81 ± 0.18[ab] (6)	0.70 ± 0.13[b] (7)
Diacylglycerol acyltransferase-2 (*Dgat2*)	1.00 ± 0.08[a] (6)	1.04 ± 0.15[a] (6)	0.85 ± 0.11[b] (5)
CD36 (Cd36)	1.06 ± 0.41 (6)		0.83 ± 0.31 (6)
Lipolysis and fatty acid oxidation			

Table 3. Relative Expression of mRNAs in the liver

Genes	wt	pai/wt	pai/pai
Hepatic triglyceride lipase (*Htgl*)	0.98 ± 0.27 (7)	0.90 ± 0.28 (6)	1.13 ± 0.34 (7)
Adipose triglyceride lipase (*Atgl*)	1.02 ± 0.21[a] (6)	0.79 ± 0.36[ab] (6)	0.56 ± 0.14[b] (6)
Hormone-sensitive lipase (*Hsl*)	1.05 ± 0.33 (8)	1.29 ± 0.41 (6)	1.16 ± 0.49 (8)
Monoacylglycerol lipase (*Mgl*)	1.02 ± 0.19[a] (8)	1.65 ± 0.55[b] (6)	1.56 ± 0.58[b] (7)
Comparative gene identification 58 (*Cgi58*)	1.05 ± 0.34[a] (7)	1.38 ± 0.66[ab] (6)	1.75 ± 0.59[b] (7)
Adenylate cyclase 3 (*Adcy3*)	1.07 ± 0.42 (8)		1.08 ± 0.23 (8)
Lipoprotein lipase (*Lpl*)	1.02 ± 0.23[a] (7)	0.60 ± 0.17[b] (6)	0.50 ± 0.23[b] (6)
Carnitine palmitoyltransferase Ia (*Cpt1a*)	1.01 ± 0.19[a] (14)	0.83 ± 0.17[b] (7)	0.68 ± 0.18[b] (11)
Long-chain 3-hydroxyacyl-CoA dehydrogenase (*Lchad*)	1.04 ± 0.28 (9)		1.01 ± 0.25 (9)
Acetyl-CoA acyltransferase 2 (*Acaa2*)	1.08 ± 0.44 (7)		1.23 ± 0.23 (6)
Long-chain acyl-CoA dehydrogenase (*Lcad*)	1.00 ± 0.09 (8)	0.93 ± 0.22 (7)	0.78 ± 0.30 (8)
Medium-chain acyl-CoA dehydrogenase (*Mcad*)	1.03 ± 0.27[a] (9)	0.57 ± 0.12[b] (6)	0.65 ± 0.20[b] (6)
Uncoupling protein 1 (*Ucp1*)	1.04 ± 0.32 (7)	1.12 ± 0.40 (7)	0.98 ± 0.34 (7)
Acyl-CoA oxidase-1 (*Acox1*)	1.04 ± 0.32[a] (8)	0.89 ± 0.32[a] (7)	0.69 ± 0.32[b] (8)
Acyl-CoA oxidase-2 (*Acox2*)	1.07 ± 0.42 (9)		1.17 ± 0.43 (9)
Insulin and IGF-1 signaling			
Insulin receptor (*Insr*)	1.05 ± 0.37 (9)	1.35 ± 0.42 (6)	1.36 ± 0.70 (8)
Insulin receptor substrate-1 (*Irs1*)	0.97 ± 0.43 (6)	0.97 ± 0.43 (4)	0.94 ± 0.59 (6)
Insulin receptor substrate-2 (*Irs2*)	1.27 ± 1.01 (9)	1.27 ± 0.87 (7)	1.41 ± 0.99 (8)
Phosphoinositide 3-kinase (*Pi3k*)	1.04 ± 0.28 (7)		1.17 ± 0.24 (7)
Insulin-like growth factor-1 (*Igf1*)	1.04 ± 0.31[a] (8)	1.16 ± 0.29[a] (7)	2.09 ± 0.80[b] (6)
IGF binding protein 1 (*Igfbp1*)	1.04 ± 0.30[a] (6)	0.45 ± 0.33[b] (6)	0.09 ± 0.02[b] (5)
Forkhead box protein a2 (*Foxa2*)	1.06 ± 0.37[a] (9)	1.98 ± 0.86[b] (6)	1.76 ± 0.48[b] (7)
Glucose metabolism and gluconeogenesis			
Glucose transporter type 4 (*Glut4*)	1.06 ± 0.38[a] (6)	0.88 ± 0.28[a] (5)	0.61 ± 0.25[b] (6)
Carbohydrate response element binding protein (*Chrebp*)	1.03 ± 0.26 (5)		1.33 ± 0.43 (6)
Fibroblast growth factor 21 (*Fgf21*)	1.07 ± 0.46[a] (5)		0.19 ± 0.12[b] (7)
Glucose-6-phosphatase (*G6p*)	1.07 ± 0.41[a] (9)	0.47 ± 0.17[b] (7)	0.66 ± 0.19[b] (6)
Phosphoenolpyruvate carboxykinase (*Pepck*)	1.04 ± 0.29[a] (8)	0.53 ± 0.22[b] (6)	0.51 ± 0.19[b] (7)
NADPH-producing			
Malic enzyme (*Malic*)	0.99 ± 0.32[a] (8)	0.98 ± 0.39[a] (7)	1.72 ± 0.70[b] (7)
Glucose-6-phosphate dehydrogenase (*G6pd*)	1.06 ± 0.38 (6)	1.14 ± 0.34 (4)	1.05 ± 0.46 (4)
6-Phosphogluconate dehydrogenase (*Pgd*)	1.05 ± 0.35[a] (7)		1.73 ± 0.56[b] (6)
Others			
AMP-activated protein kinase (*Ampk*)	1.07 ± 0.41 (7)		1.48 ± 0.32 (7)
Liver kinase B1 (*Lkb1*)	1.02 ± 0.23 (5)		1.10 ± 0.12 (5)

Table 3. Relative Expression of mRNAs in the liver

Genes	wt	pai/wt	pai/pai
Nuclear receptor subfamily 3 group C member 1 (*Nr3c1*)	1.07 ± 0.39 (6)		2.01 ± 1.05 (6)
CD11c	1.04 ± 0.31[a] (7)	0.57 ± 0.26[b] (6)	0.53 ± 0.27[b] (7)
Cyclophilin	1.01 ± 0.17 (9)	1.04 ± 0.28 (6)	1.01 ± 0.16 (6)
Pai	1.01 ± 0.43[a] (5)	1674 ± 569[b] (6)	6059 ± 2317[c] (6)

Numbers in brackets indicate the size of tested samples. Each value represents the mean ± SD. Different letters in superscript indicate $p < 0.05$.

386

387 Compared to wt samples, pai/wt livers exhibited normal except for swollen
388 cells (Fig. 6 E). However, among the forty tested genes (Table 3), the mRNA levels of
389 eight genes (Hmgcr, Ldlr, Ppar-γ, Dgat2, Acox1, Igf1, Glut4, and Malic) were
390 significantly ($p < 0.05$) different from those in pai/pai livers, but not different from
391 those in wt samples. The remaining 32 genes had similar transcription levels to
392 pai/pai samples, and 13 (33%) of them were markedly different from those in wt
393 samples ($p < 0.05$). Specifically, these 13 genes that exhibited different expressions
394 from wt livers included four up-regulated (Mgl, Srebp1c, Insig1, and Foxa2) and nine
395 down-regulated (Lpl, Cpt1a, Mcad, Srebp1a, Insig2, Igfbp1, G6p, Pepck, and Cd11c).
396 These results suggest that gene expression is genotype-specific and that the process of
397 lipolysis and gluconeogenesis is impaired in pai/wt mice.

398

399 ***3. 8. Hypothalamic analysis***

400 To determine whether t10c12-CLA affected the hypothalamus, critical
401 hypothalamic genes and proteins were also measured. The mRNA levels of the leptin
402 receptor and agouti-related peptide were increased, while the transcription levels of
403 the ghrelin receptor and Orexins decreased in the pai/wt or pai/pai hypothalamus
404 when compared to wt mice (Fig. 7 A). Western blot analysis revealed no changes in
405 AMPK, phosphorylated AMPK, and GRP78 proteins in the pai/pai hypothalamus,
406 additionally, the ratio of pAMPK/AMPK did not show a significant difference
407 between wt and pai/pai samples ($p > 0.05$; Fig. 7 B-C). These findings suggest that the
408 central regulation of energy intake may only be affected at the transcriptional level.

409

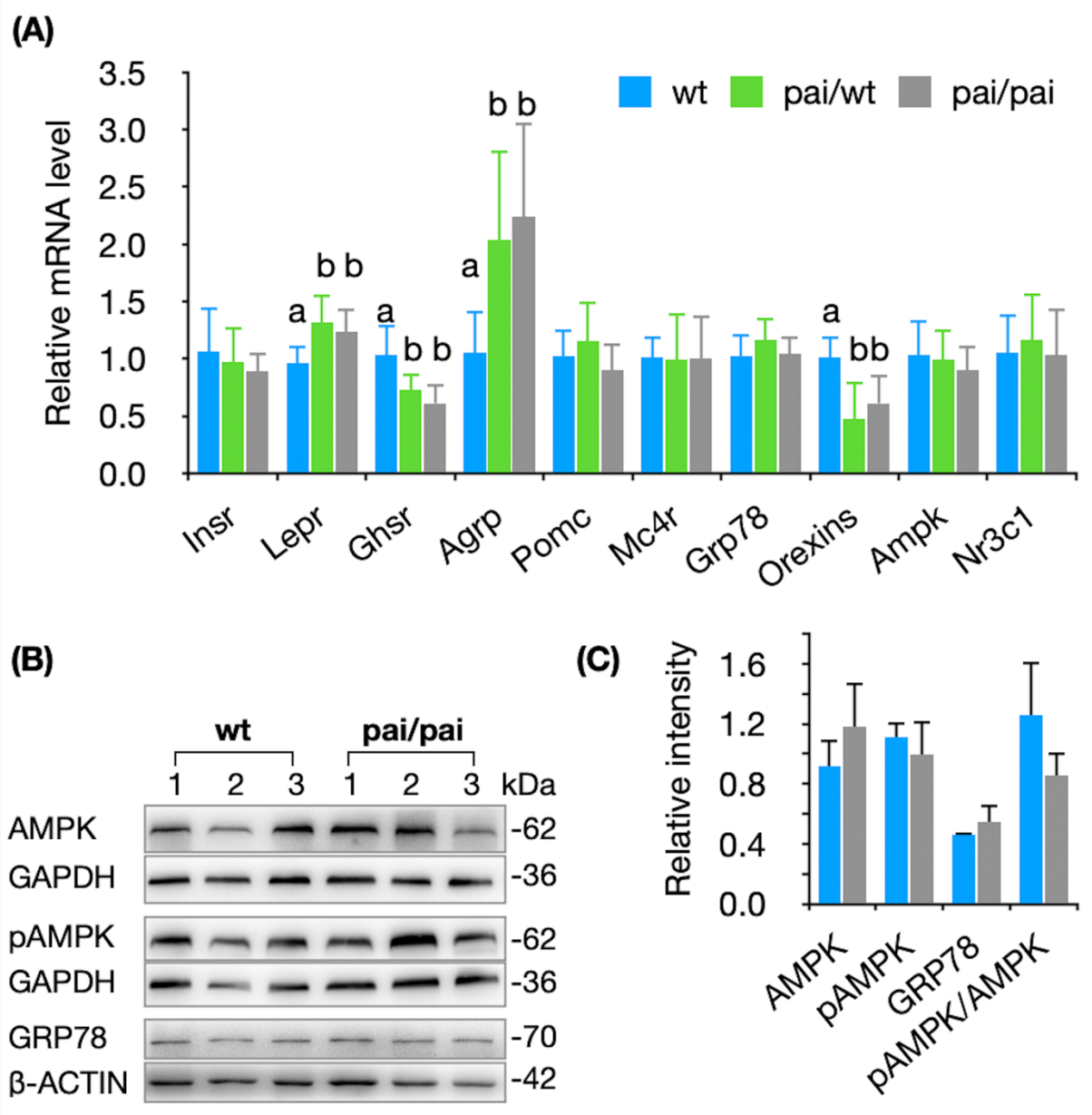

Figure 7. Analyses of the relative mRNAs (A), proteins levels and their relative intensities in the hypothalamus (B-C). Agrp, Agouti-related peptide; Ampk, AMP-activated protein kinase; Ghsr, Ghrelin receptor; Grp78, glucose-regulated protein 78; Insr, Insulin receptor; Lepr, Leptin receptor; Mc4r, Melanocortic 4 receptor; Nr3c1, Nuclear receptor subfamily 3 group C member 1; (p)AMPK, (phosphorylated) AMP-activated protein kinase; Pomc, Proopiomelanocortin. The sample sizes for RNA analysis are 6~9 in each group. The bars represent the mean ± SD. Different letters indicate $p < 0.05$.

418 **4. DISCUSSION**

419

420 It has been reported that t10c12-CLA can depress milk fat production by
421 inhibiting lipogenesis [5-7], reducing the globule size of milk fat droplets [8]. A study
422 on grazing herds indicated that other fatty acids, apart from t10c12-CLA, may also
423 inhibit milk fat synthesis during milk fat depression [18]. These results suggest that
424 this milk fat depression may result from t10c12-CLA directly or other compositions
425 induced by t10c12-CLA indirectly. Research on early-weaning lambs has revealed that
426 t10c12-CLA can facilitate the weaning transition through the microbiota-host
427 transcriptome interaction [19]. In the current study, maternal t10c12-CLA plays an
428 active role in development in female offspring, similar to male offspring fostered by
429 pai/wt mother (Rao et al, 2023 bioRxiv preprint:
430 https://doi.org/10.1101/2023.01.31.526123). It suggests that maternal t10c12-CLA
431 benefits embryo and/or offspring development.

432 Our previous observation showed that t10c12-CLA reduced body fat by
433 releasing heat via BAT activation in pai/pai male mice with lower blood TGs (Rao et
434 al, 2023 bioRxiv preprint: https://doi.org/10.1101/2023.01.31.526123). Conversely, in
435 the pai female mice, t10c12-CLA did not cause body fat loss but resulted in
436 complicated symptoms, including hypothermia, fatty liver and hypertriglyceridemia,
437 and highly responsive to stress and inflammation in a dose-dependent manner. The
438 different physiological and pathological characteristics of both sexes can help us
439 understand the mechanism of action of t10c12-CLA in gender-specific and dose-
440 dependent manners. As for pai mice, there are two problems we have not fixed until
441 now. Firstly, we have reported as many results as possible for a comprehensive
442 understanding of the pai mouse, but a few parameters are difficult to be explained
443 well, and even show contradictions in some respects. Secondly, explaining why there
444 are only minimal differences in t10c12-CLA and linoleic acid is challenging although
445 we once observed drastic changes in an increase of product t10c12-CLA and a decrease
446 of substrate linoleic acid in pai-transfected 3T3 cells [18].

447 The metabolic pathway of t10c12-CLA, similar to that of linoleic or alpha-
448 linolenic acids [20], suggests it can competitively interrupt the metabolic pathway of
449 n-6 or n-3 FAs and their derived leukotrienes signals/hormonal molecules. It also
450 indicates that t10c12-CLA can be directly converted into the analogues of n-6 FAs and
451 their derivatives. PGE2, an arachidonic acid-derived hormone, will be easily disturbed

452 by t10c12-CLA. PGE2 is involved in stress response and has essential effects on
453 inflammation, fever, and renal filtration [21]. It can induce corticosterone secretion by
454 regulating the hypothalamic-pituitary-adrenal axis activity and enhancing adrenaline
455 synthesis in the Chromaffin cells of the adrenal medulla. Subsequently, the increased
456 circulating corticosterone and adrenaline could stimulate excess glucagon secretion
457 [22]. In pai/pai female mice, we have observed the excess PGE2 induced by t10c12-
458 CLA, and then the PGE2 (or analogues) caused the increases in corticosterone,
459 glucagon, adrenaline, and inflammatory factors (IL-6, TNFα, and CRP). Obviously,
460 hypothermia in pai/pai female mice may be related to hyperprostaglandinemia,
461 hyperadrenerginemia and inflammatory response; while hyperglyceridemia and fatty
462 liver are associated with hypercorticosteroidemia and glucagon resistance.

463 In the hypothalamic preoptic area, PGE2 receptors EP3, coupled to cAMP
464 decreases, can stimulate a passive defence mechanism such as less O_2 consumption
465 and hypothermia to avoid further energy expenditure; while receptors EP4, connected
466 to cAMP increases, can stimulate an active defence mechanism, including more O_2
467 consumption and febrile responses by increasing BAT thermogenesis, typically occurs
468 to promote well-being and survival [21,23]. It suggests that gender-based differences
469 in PGE2 levels might partially result in the opposite heat release in male and female
470 pai/pai mice. In female mice, the co-elevation of PGE2 and corticosterone suggests
471 that t10c12-CLA induced a passive defence mechanism including hypothermia which
472 conversely promote BAT thermogenesis and lipid metabolism by negative feedback
473 to down-regulate pAMPK and up-regulate UCP1, UCP2, CPT1B, and pHSL. In
474 contrast, in male mice, the lack of PGE2 elevation suggests that t10c12-CLA induced
475 an active defence mechanism including hyperthermia to promote survival (Rao et al,
476 2023 bioRxiv preprint: https://doi.org/10.1101/2023.01.31.526123).

477 In addition to PGE2- and adrenaline-induced heating [24], BAT thermogenesis
478 can be mediated through the central GRP78 [25,26] or AMPK-OREXINS-BMP8B
479 pathway [27]. Orexin-null mice exhibited periods of decreased activity during the dark
480 phase and demonstrated hypothermia, reduced oxygen consumption, and blunted
481 thermogenic responses [28]; furthermore, BMP8B's thermogenic effect is sexually
482 dimorphic and observed in females only [27]. The pai/pai female mice exhibited
483 similar phenotypes to orexin-null mice and lower transcription levels of Orexins in
484 the pai hypothalamus. These characteristics suggest that the t10c12-CLA-induced
485 BAT thermogenesis may be regulated through central pathways in female mice.

486 Unfortunately, we did not observe evident changes in GRP78, AMPK, pAMPK, and
487 pAMPK/AMPK ratio in the hypothalamus.

488 Previous studies on mice have yielded conflicting results on whether dietary
489 t10c12-CLA leads to hepatic steatosis [15,29-31]. The current observation of fatty liver
490 and hypertriglyceridemia in pai/pai mice, which may be associated with t10c12-CLA-
491 induced excess corticosterone for the overproduction of corticosterone can lead to
492 Cushing syndrome, corticosteroid-induced lipodystrophy, hypertriglyceridemia, or
493 hepatic steatosis [32,33]. On the other hand, the existence of glucagon resistance can
494 increase liver fat [34-36], although chronic increases in plasma glucagon promote
495 lipolysis through INSP3R1/CAMKII/ATGL [37] or PKA/HSL pathways in
496 hepatocytes [38] and stimulate beta-oxidation by activating AMPK/PPAR-
497 α/CPT1A/MCAD pathway [22]. In the current study, the serum glucagon
498 concentration increased nearly twofold in pai/pai female mice, which is similar to its
499 physiological levels (2~3 fold) in response to long-term fasting or hypoglycemia [39],
500 whereas the protein levels of unchanged ATGL, decreased pAMPK, and increased
501 CPT1A indicate the chronic glucagon excess did not stimulate the lipolysis and beta-
502 oxidation in the liver. These results suggest that the chronic impact of t10c12-CLA
503 might give rise to glucagon resistance in pai/pai female mice. In this case, the down-
504 regulated hepatic enzymes may not fully and immediately catalyse the FAs molecules
505 mobilised from other tissues based on glucagon stimulation. Consequently, it disrupts
506 hepatic and systemic lipid homeostasis and leads to dyslipidemia and fatty liver in
507 female mice. Contrarily, the t10c12-CLA did not cause the overproduction of
508 corticosterone or glucagon in pai/pai male mice, thus, the mice had no fatty liver
509 disease and even exhibited lower TGs levels in the blood.

510 FGF21 is a key regulator of the specific hormonal signalling pathway in
511 increasing energy expenditure, reducing hepatic and plasma TGs levels, accelerating
512 lipoprotein catabolism in WAT and BAT [40], and suppressing physical activity via
513 central action [41]. FGF21 signalling enhances insulin sensitivity and lowers serum
514 glucose by acting directly on adipose tissues [17,42]. As we know, the pai/wt mouse is
515 the first animal that t10c12-CLA can induce FGF21 secretion. Excess FGF21 is a unique
516 feature in pai/wt, not in pai/pai genotypes, indicating that t10c12-CLA-induced
517 FGF21 secretion is specifically associated with low doses in both genders and it can be
518 suppressed to the normal levels through negative feedback when high doses occurred
519 in pai/pai mice. This suggests that the health benefits of low-dose t10c12-CLA may be

520 due, in part, to its ability to stimulate FGF21 secretion. Therefore, the different effects
521 of t10c12-CLA on glucose metabolism in diabetic Zucker fatty rats [43] and insulin
522 resistance in mice [44,45] may be related to the different levels of FGF21 induced by
523 t10c12-CLA. In the current study, excess FGF21 may be associated with specific
524 phenotypes in pai/wt mice, such as blood glucose homeostasis during starvation,
525 enlarged white adipocytes, no steatosis in hepatocytes and normal circulating TGs.
526 The exact mechanism by which t10c12-CLA activates FGF21 secretion remains unclear
527 and requires further investigation.

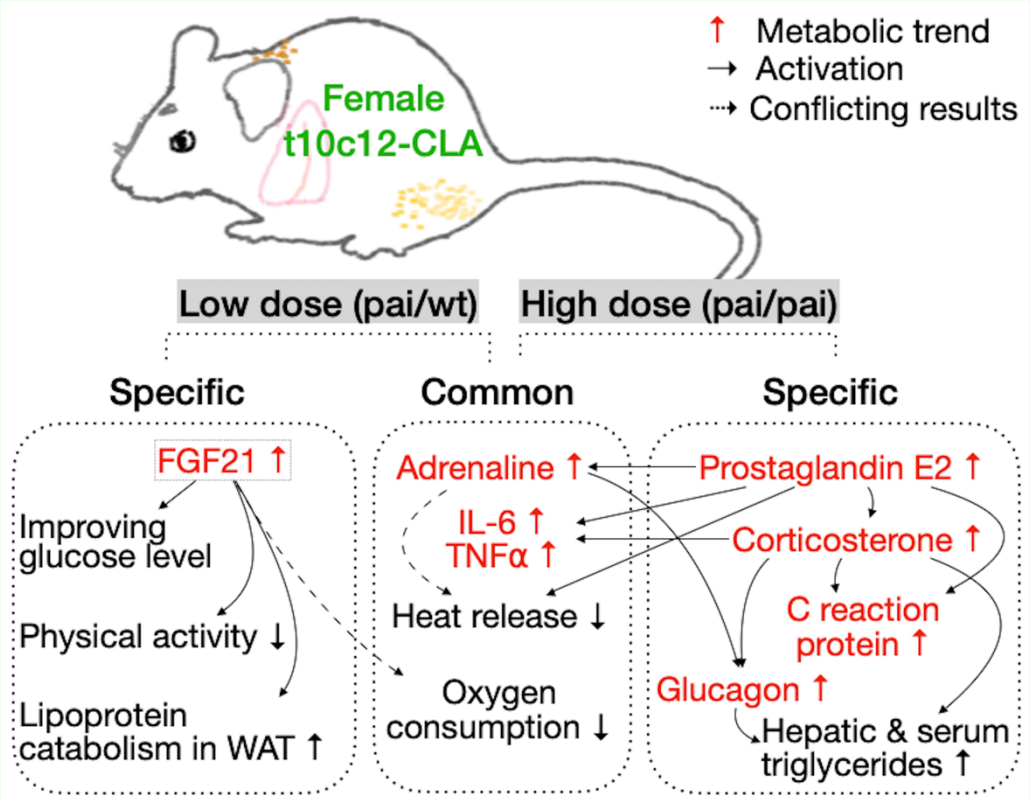

528 **Figure 8. Diagram showing the dose-dependent effect of chronic t10c12-CLA on lean**
529 **female mice**. Besides the common effects, such as increased adrenaline, IL-6, and TNFα, as
530 well as decreased heat release and oxygen consumption (Middle panel), the low doses
531 specifically increase circulating levels of FGF21 which plays active roles in maintaining
532 energy homeostasis, suppressing physical activity, and improving serum glucose levels in
533 pai/wt mice (Left panel). Conversely, the high doses specifically result in excesses of
534 prostaglandin E2, corticosterone, glucagon, and C reaction protein; subsequently, the
535 combination of these factors causes metabolic syndrome, including hypothermia, fatty liver,
536 and hypertriglyceridemia in pai/pai mice (Right panel). Words in black and red describe
537 physiological features and endocrinal factors, respectively.

538

539 Based on the observation in female animals in this study, we suggest that low
540 doses of t10c12-CLA may cause increases in circulating adrenaline which can induce
541 WAT lipolysis and BAT heating through a mechanism of negative feedback, and
542 FGF21 which can promote energy expenditure, reduce hepatic and plasma TGs levels,
543 accelerate lipoprotein catabolism in adipocytes, suppress physical activity, and
544 enhance insulin sensitivity and lower serum glucose (as shown in Fig. 8). Conversely,
545 high doses of t10c12 results in an increased PEG2 which induces increases in
546 corticosterone, glucagon, adrenaline, and inflammatory factors. The combination of
547 these factors causes metabolic syndrome, including fatty liver and hyperglyceridemia,
548 hyperprostaglandinemia and hypothermia, and inflammatory changes in female mice
549 (as shown in Fig. 8). The metabolic impact of t10c12-CLA involves various hormones
550 and inflammatory factors and is system-wide effects on multiple metabolic pathways.
551 Thus, interpreting the data from pai mice requires careful consideration, and more
552 work is needed to understand the mechanism of action of t10c12-CLA and its
553 metabolic impact.

554 Totally, our results suggest that the chronic effects of t10c12-CLA on lean
555 animals are dose-dependent and differ between sexes and low doses of t10c12-CLA
556 are beneficial while high doses may become a health risk in lean female mammals.
557 Further research is necessary to understand the health benefits and safety risks of
558 t10c12-CLA on pai obese mice.

559

560 **Abbreviations**

561 t10c12-CLA, trans 10, cis 12-conjugated linoleic acid; LA, linoleic aci; pai,
562 Propionibacterium acnes isomerase; wt, wild-type; FGF21, fibroblast growth factor 21;
563 UCP, uncoupling protein; AMPK, AMP-activated protein kinase; pAMPK,
564 phosphorylated AMPK; HSL, hormone-sensitive lipase; pHSL, phosphorylated HSL;
565 CPT1, carnitine palmitoyltransferase I; BAT, brown adipose tissue; WAT, white
566 adipose tissue; FAs, fatty acids

567 **Ethics approval and consent to participate:**

568 All animal experiments followed the Committee for Experimental Animals of
569 Yangzhou University.

570 **Institutional Review Board Statement:**

571 The animal study protocol was approved by the Ethics Committee of
572 Yangzhou University (protocol code NSFC2020-SYXY-20 and dated 25 March 2020).

573 **Consent for publication:**

574 Not applicable

575 **Availability of data and materials:**

576 The datasets used and/or analysed during the current study are available
577 from the corresponding author upon reasonable request.

578 **Competing interests:**

579 The authors declare that they have no competing interests.

580 **Funding sources**

581 This work was supported by the National Key Research and Development
582 Program of China (2018YFC1003800), the Project Funded by the Priority Academic
583 Program Development of Jiangsu Higher Education Institutions (PAPD), and Jiangsu
584 Funding Program for Excellent Postdoctoral Talent (Rao Y).

585 **Acknowledgement**

586 We thank graduate students Qi Wang, Mei Liu, and Jiaqi Lu in our lab for their
587 generous assistance in partial tests and Ms Yuyang Wang in our university for
588 technique help in gas chromatography. We also thank Professor Hongjun Wang at the
589 Medical University of South Carolina, USA, for the helpful discussion during the
590 writing process and Ms Wenjing Gou's language assistance in preparing this
591 manuscript.

592 **Authors 'contributions:**

593 Conceptualization, Y Rao and K Gou; Data curation, Y Rao, M Li, B Wang, Y
594 Wang, and L Liang; Formal analysis, Y Rao and K Gou; Funding acquisition, Y Rao
595 and K Gou; Investigation, Y Rao, M Li, B Wang, Y Wang and L Liang; Methodology,
596 Y Rao, M Li, B Wang, Y Wang and L Liang; Project administration, K Gou; Software,

Y Rao; Supervision, K Gou; Validation, K Gou; Visualization, Y Rao and L Liang; Writing – original draft, Y Rao; Writing – review & editing, K Gou. All authors proofread, made comments, and approved the report.

Supplementary data

This manuscript contains supplementary data.

References

1. Shen, W.; Baldwin, J.; Collins, B.; Hixson, L.; Lee, K.T.; Herberg, T.; Stames, J.; Cooney, P.; Chuang, C.C.; Hopkins, R., et al. Low level of trans-10, cis-12 conjugated linoleic acid decreases adiposity and increases browning independent of inflammatory signaling in overweight Sv129 mice. *Journal of Nutritional Biochemistry* **2015**, *26*, 616-625, doi:10.1016/j.jnutbio.2014.12.016.

2. den Hartigh, L.J.; Wang, S.R.; Goodspeed, L.; Wietecha, T.; Houston, B.; Omer, M.; Ogimoto, K.; Subramanian, S.; Gowda, G.A.N.; O'Brien, K.D., et al. Metabolically distinct weight loss by 10,12 CLA and caloric restriction highlight the importance of subcutaneous white adipose tissue for glucose homeostasis in mice. *Plos One* **2017**, *12*, doi:10.1371/journal.pone.0172912.

3. Berkel, C.; Cacan, E. Trans-10, cis-12 conjugated linoleic acid- and caloric restriction-mediated upregulation of CNDP2 expression in white adipose tissue in rodents, with implications in feeding and obesity. *J Nutr Biochem* **2023**, *114*, 109269, doi:10.1016/j.jnutbio.2023.109269.

4. Wang, L.; Zhang, S.; Huang, Y.; You, W.; Zhou, Y.; Chen, W.; Sun, Y.; Yi, W.; Sun, H.; Xie, J., et al. CLA improves the lipo-nutritional quality of

621 pork and regulates the gut microbiota in Heigai pigs. *Food Funct* **2022**,
622 *13*, 12093-12104, doi:10.1039/d2fo02549c.

623 5. Baumgard, L.H.; Sangster, J.K.; Bauman, D.E. Milk fat synthesis in dairy
624 cows is progressively reduced by increasing supplemental amounts of
625 trans-10, cis-12 conjugated linoleic acid (CLA). *J Nutr* **2001**, *131*, 1764-
626 1769, doi:10.1093/jn/131.6.1764.

627 6. Harvatine, K.J.; Robblee, M.M.; Thorn, S.R.; Boisclair, Y.R.; Bauman, D.E.
628 Trans-10, cis-12 CLA dose-dependently inhibits milk fat synthesis without
629 disruption of lactation in C57BL/6J mice. *J Nutr* **2014**, *144*, 1928-1934,
630 doi:10.3945/jn.114.198911.

631 7. Harvatine, K.J.; Boisclair, Y.R.; Bauman, D.E. Time-dependent effect of
632 trans-10,cis-12 conjugated linoleic acid on gene expression of lipogenic
633 enzymes and regulators in mammary tissue of dairy cows. *J Dairy Sci*
634 **2018**, *101*, 7585-7592, doi:10.3168/jds.2017-13935.

635 8. Han, L.; Huang, Q.; Yang, J.; Lu, W.; Hu, M.; Yang, Y.; Zhu, H.; Pang, K.;
636 Yang, G. Proteomic analysis of milk fat globule membranes from small-
637 sized milk fat globules and their function in promoting lipid droplet
638 fusion in bovine mammary epithelial cells. *Food Funct* **2023**, *14*, 2304-
639 2312, doi:10.1039/d2fo03476j.

640 9. Kanter, J.E.; Goodspeed, L.; Wang, S.; Kramer, F.; Wietecha, T.; Gomes-
641 Kjerulf, D.; Subramanian, S.; O'Brien, K.D.; den Hartigh, L.J. 10,12
642 Conjugated Linoleic Acid-Driven Weight Loss Is Protective against
643 Atherosclerosis in Mice and Is Associated with Alternative Macrophage
644 Enrichment in Perivascular Adipose Tissue. *Nutrients* **2018**, *10*,
645 doi:10.3390/nu10101416.

646 10. Vaisar, T.; Wang, S.; Omer, M.; Irwin, A.D.; Storey, C.; Tang, C.; den
647 Hartigh, L.J. 10,12-Conjugated linoleic acid supplementation improves
648 HDL composition and function in mice. *J Lipid Res* **2022**, *63*, 100241,
649 doi:10.1016/j.jlr.2022.100241.

650 11. Kim, J.H.; Kim, Y.; Kim, Y.J.; Park, Y. Conjugated linoleic acid: Potential
651 health benefits as a functional food ingredient. *Annu Rev Food Sci*
652 *Technol* **2016**, *7*, 221-244, doi:10.1146/annurev-food-041715-033028.

653 12. Marques, T.M.; Wall, R.; O'Sullivan, O.; Fitzgerald, G.F.; Shanahan, F.;
654 Quigley, E.M.; Cotter, P.D.; Cryan, J.F.; Dinan, T.G.; Ross, R.P., et al.
655 Dietary trans-10, cis-12-conjugated linoleic acid alters fatty acid
656 metabolism and microbiota composition in mice. *Br J Nutr* **2015**, *113*,
657 728-738, doi:10.1017/S0007114514004206.

658 13. Cuciniello, R.; Luongo, D.; Ferramosca, A.; Lunetti, P.; Rotondi-Aufiero,
659 V.; Crispi, S.; Zara, V.; Maurano, F.; Filosa, S.; Bergamo, P. Conjugated
660 linoleic acid downregulates Alzheimer's hallmarks in aluminum mouse
661 model through an Nrf2-mediated adaptive response and increases brain
662 glucose transporter levels. *Free Radic Biol Med* **2022**, *191*, 48-58,
663 doi:10.1016/j.freeradbiomed.2022.08.027.

664 14. Sisk, M.B.; Hausman, D.B.; Martin, R.J.; Azain, M.J. Dietary conjugated
665 linoleic acid reduces adiposity in lean but not obese Zucker rats. *J Nutr*
666 **2001**, *131*, 1668-1674, doi:10.1093/jn/131.6.1668.

667 15. Li, S.L.; Ma, S.Y.; Xu, B.R.; Fan, Z.Y.; Li, M.J.; Cao, W.G.; Gou, K.M.
668 Effects of trans-10, cis-12-conjugated linoleic acid on mice are influenced
669 by the dietary fat content and the degree of murine obesity. *Eur J Lipid*
670 *Sci Tech* **2015**, *117*, 1908-1918, doi:10.1002/ejlt.201400568.

671 16. den Hartigh, L.J. Conjugated Linoleic Acid Effects on Cancer, Obesity,
672 and Atherosclerosis: A Review of Pre-Clinical and Human Trials with
673 Current Perspectives. *Nutrients* **2019**, *11*, doi:10.3390/nu11020370.

674 17. Flippo, K.H.; Potthoff, M.J. Metabolic Messengers: FGF21. *Nat Metab*
675 **2021**, *3*, 309-317, doi:10.1038/s42255-021-00354-2.

676 18. Neville, O.B.; Fahey, A.G.; Mulligan, F.J. Comparison of milk and grass
677 composition from grazing Irish dairy herds with and without milk fat
678 depression. *Ir Vet J* **2023**, *76*, 5, doi:10.1186/s13620-023-00230-3.

679 19. Yang, C.; Deng, X.; Lund, P.; Liu, H.; Ding, X.; Fu, Z.; Zhang, N.; Li, J.;
680 Dong, L. Rumen microbiota-host transcriptome interaction mediates the
681 protective effects of trans-10, cis-12 CLA on facilitating weaning
682 transition of lambs. *Anim Nutr* **2023**, *12*, 345-359,
683 doi:10.1016/j.aninu.2022.11.002.

684 20. Subbaiah, P.V.; Gould, I.G.; Lal, S.; Aizezi, B. Incorporation profiles of
685 conjugated linoleic acid isomers in cell membranes and their positional
686 distribution in phospholipids. *Biochim Biophys Acta* **2011**, *1811*, 17-24,
687 doi:10.1016/j.bbalip.2010.09.004.

688 21. Furuyashiki, T.; Narumiya, S. Stress responses: the contribution of
689 prostaglandin E(2) and its receptors. *Nat Rev Endocrinol* **2011**, *7*, 163-
690 175, doi:10.1038/nrendo.2010.194.

691 22. Zeigerer, A.; Sekar, R.; Kleinert, M.; Nason, S.; Habegger, K.M.; Muller,
692 T.D. Glucagon's metabolic action in health and disease. *Compr Physiol*
693 **2021**, *11*, 1759-1783, doi:10.1002/cphy.c200013.

694 23. Saper, C.B.; Lowell, B.B. The hypothalamus. *Curr Biol* **2014**, *24*, R1111-
695 1116, doi:10.1016/j.cub.2014.10.023.

696 24. Cypess, A.M.; Weiner, L.S.; Roberts-Toler, C.; Franquet Elia, E.; Kessler,
697 S.H.; Kahn, P.A.; English, J.; Chatman, K.; Trauger, S.A.; Doria, A., et al.
698 Activation of human brown adipose tissue by a beta3-adrenergic receptor
699 agonist. *Cell Metab* **2015**, *21*, 33-38, doi:10.1016/j.cmet.2014.12.009.

700 25. Contreras, C.; Gonzalez-Garcia, I.; Seoane-Collazo, P.; Martinez-Sanchez,
701 N.; Linares-Pose, L.; Rial-Pensado, E.; Ferno, J.; Tena-Sempere, M.;
702 Casals, N.; Dieguez, C., et al. Reduction of hypothalamic endoplasmic
703 reticulum stress activates browning of white fat and ameliorates obesity.
704 *Diabetes* **2017**, *66*, 87-99, doi:10.2337/db15-1547.

705 26. Contreras, C.; Fondevila, M.F.; Lopez, M. Hypothalamic GRP78, a new
706 target against obesity? *Adipocyte* **2018**, *7*, 63-66,
707 doi:10.1080/21623945.2017.1405878.

708 27. Martins, L.; Seoane-Collazo, P.; Contreras, C.; Gonzalez-Garcia, I.;
709 Martinez-Sanchez, N.; Gonzalez, F.; Zalvide, J.; Gallego, R.; Dieguez, C.;
710 Nogueiras, R., et al. A functional link between ampk and orexin mediates
711 the effect of bmp8b on energy balance. *Cell Rep* **2016**, *16*, 2231-2242,
712 doi:10.1016/j.celrep.2016.07.045.

713 28. Chemelli, R.M.; Willie, J.T.; Sinton, C.M.; Elmquist, J.K.; Scammell, T.; Lee,
714 C.; Richardson, J.A.; Williams, S.C.; Xiong, Y.M.; Kisanuki, Y., et al.
715 Narcolepsy in orexin knockout mice: Molecular genetics of sleep
716 regulation. *Cell* **1999**, *98*, 437-451, doi:Doi 10.1016/S0092-8674(00)81973-
717 X.

718 29. Ashwell, M.S.; Ceddia, R.P.; House, R.L.; Cassady, J.P.; Eisen, E.J.; Eling,
719 T.E.; Collins, J.B.; Grissom, S.F.; Odle, J. Trans-10, cis-12-conjugated
720 linoleic acid alters hepatic gene expression in a polygenic obese line of

721 mice displaying hepatic lipidosis. *J Nutr Biochem* **2010**, *21*, 848-855,
722 doi:10.1016/j.jnutbio.2009.06.013.

723 30. Vyas, D.; Kadegowda, A.K.; Erdman, R.A. Dietary conjugated linoleic
724 acid and hepatic steatosis: species-specific effects on liver and adipose
725 lipid metabolism and gene expression. *J Nutr Metab* **2012**, *2012*, 932928,
726 doi:10.1155/2012/932928.

727 31. Cordoba-Chacon, J.; Sugasini, D.; Yalagala, P.C.R.; Tummala, A.; White,
728 Z.C.; Nagao, T.; Kineman, R.D.; Subbaiah, P.V. Tissue-dependent effects
729 of cis-9,trans-11- and trans-10,cis-12-CLA isomers on glucose and lipid
730 metabolism in adult male mice. *J Nutr Biochem* **2019**, *67*, 90-100,
731 doi:10.1016/j.jnutbio.2019.01.020.

732 32. Laryea, G.; Schutz, G.; Muglia, L.J. Disrupting hypothalamic
733 glucocorticoid receptors causes HPA axis hyperactivity and excess
734 adiposity. *Mol Endocrinol* **2013**, *27*, 1655-1665, doi:10.1210/me.2013-
735 1187.

736 33. Nicolaides, N.C.; Charmandari, E.; Kino, T.; Chrousos, G.P. Stress-related
737 and circadian secretion and target tissue actions of glucocorticoids:
738 Impact on health. *Front Endocrinol (Lausanne)* **2017**, *8*, 70,
739 doi:10.3389/fendo.2017.00070.

740 34. Krilov, L.; Nguyen, A.; Miyazaki, T.; Unson, C.G.; Bouscarel, B. Glucagon
741 receptor recycling: role of carboxyl terminus, beta-arrestins, and
742 cytoskeleton. *Am J Physiol-Cell Ph* **2008**, *295*, C1230-C1237,
743 doi:10.1152/ajpcell.00240.2008.

744 35. Charbonneau, A.; Unson, C.G.; Lavoie, J.M. High-fat diet-induced hepatic
745 steatosis reduces glucagon receptor content in rat hepatocytes: potential

746 interaction with acute exercise. *J Physiol-London* **2007**, *579*, 255-267,
747 doi:10.1113/jphysiol.2006.121954.

748 36. Sammons, M.F.; Lee, E.C.Y. Recent progress in the development of small-
749 molecule glucagon receptor antagonists. *Bioorg Med Chem Lett* **2015**, *25*,
750 4057-4064, doi:10.1016/j.bmcl.2015.07.092.

751 37. Perry, R.J.; Zhang, D.; Guerra, M.T.; Brill, A.L.; Goedeke, L.; Nasiri, A.R.;
752 Rabin-Court, A.; Wang, Y.; Peng, L.; Dufour, S., et al. Glucagon stimulates
753 gluconeogenesis by INSP3R1-mediated hepatic lipolysis. *Nature* **2020**,
754 *579*, 279-283, doi:10.1038/s41586-020-2074-6.

755 38. Hayashi, Y. Glucagon regulates lipolysis and fatty acid oxidation through
756 inositol triphosphate receptor 1 in the liver. *J Diabetes Investig* **2021**, *12*,
757 32-34, doi:10.1111/jdi.13315.

758 39. Kleinert, M.; Sachs, S.; Habegger, K.M.; Hofmann, S.M.; Muller, T.D.
759 Glucagon regulation of energy expenditure. *Int J Mol Sci* **2019**, *20*,
760 doi:10.3390/ijms20215407.

761 40. Schlein, C.; Talukdar, S.; Heine, M.; Fischer, A.W.; Krott, L.M.; Nilsson,
762 S.K.; Brenner, M.B.; Heeren, J.; Scheja, L. Fgf21 lowers plasma
763 triglycerides by accelerating lipoprotein catabolism in white and brown
764 adipose tissues. *Cell Metab* **2016**, *23*, 441-453,
765 doi:10.1016/j.cmet.2016.01.006.

766 41. Bookout, A.L.; de Groot, M.H.; Owen, B.M.; Lee, S.; Gautron, L.;
767 Lawrence, H.L.; Ding, X.; Elmquist, J.K.; Takahashi, J.S.; Mangelsdorf,
768 D.J., et al. FGF21 regulates metabolism and circadian behavior by acting
769 on the nervous system. *Nat Med* **2013**, *19*, 1147-1152,
770 doi:10.1038/nm.3249.

771 42. Holland, W.L.; Adams, A.C.; Brozinick, J.T.; Bui, H.H.; Miyauchi, Y.;
772 Kusminski, C.M.; Bauer, S.M.; Wade, M.; Singhal, E.; Cheng, C.C., et al.
773 An FGF21-adiponectin-ceramide axis controls energy expenditure and
774 insulin action in mice. *Cell Metab* **2013**, *17*, 790-797,
775 doi:10.1016/j.cmet.2013.03.019.

776 43. Henriksen, E.J.; Teachey, M.K.; Taylor, Z.C.; Jacob, S.; Ptock, A.; Kramer,
777 K.; Hasselwander, O. Isomer-specific actions of conjugated linoleic acid
778 on muscle glucose transport in the obese Zucker rat. *Am J Physiol*
779 *Endocrinol Metab* **2003**, *285*, E98-E105, doi:10.1152/ajpendo.00013.2003.

780 44. Tsuboyama-Kasaoka, N.; Takahashi, M.; Tanemura, K.; Kim, H.J.; Tange,
781 T.; Okuyama, H.; Kasai, M.; Ikemoto, S.; Ezaki, O. Conjugated linoleic
782 acid supplementation reduces adipose tissue by apoptosis and develops
783 lipodystrophy in mice. *Diabetes* **2000**, *49*, 1534-1542,
784 doi:10.2337/diabetes.49.9.1534.

785 45. Clement, L.; Poirier, H.; Niot, I.; Bocher, V.; Guerre-Millo, M.; Krief, S.;
786 Staels, B.; Besnard, P. Dietary trans-10,cis-12 conjugated linoleic acid
787 induces hyperinsulinemia and fatty liver in the mouse. *J Lipid Res* **2002**,
788 *43*, 1400-1409, doi:10.1194/jlr.m20008-jlr200.

789